Prolonged dipyridamole administration reduces myocardial perfusion defects in experimental chronic Chagas cardiomyopathy

Denise Mayumi Tanaka, MS,[a] Luciano Fonseca Lemos de Oliveira, MS,[a] José Antônio Marin-Neto, PhD,[a] Minna Moreira Dias Romano, PhD,[a] Eduardo Elias Vieira de Carvalho, PhD,[b] Antonio Carlos Leite de Barros Filho, MD,[a] Fernando Fonseca França Ribeiro, MBChB, MD,[a] Jorge Mejia Cabeza, PhD,[c] Carla Duque Lopes, PhD,[a] Camila Godoy Fabricio, MS,[a] Norival Kesper, PhD,[d] Henrique Turin Moreira, PhD,[a] Lauro Wichert-Ana, PhD,[a] André Schmidt, PhD,[a] Maria de Lourdes Higuchi, PhD,[e] Edécio Cunha-Neto, PhD,[e] and Marcus Vinícius Simões, PhD[a]

[a] Medical School of Ribeirao Preto, University of São Paulo, Sao Paulo, Brazil
[b] Department of Applied Physical Therapy, Institute of Health Sciences, Federal University of Triangulo Mineiro, Minas Gerais, Brazil
[c] Hospital Israelita Albert Einstein, Sao Paulo, Brazil
[d] Instituto de Medicina Tropical, Faculty of Medicine, University os Sao Paulo, Sao Paulo, Brazil
[e] Heart Institute (InCor), Faculty of Medicine, University of Sao Paulo, Sao Paulo, Brazil

Received Oct 13, 2017; accepted Dec 20, 2017
doi:10.1007/s12350-018-1198-7

Background. **Myocardial perfusion defects (MPD) due to coronary microvascular dysfunction is frequent in chronic Chagas cardiomyopathy (CCC) and may be involved with development of myocardial damage. We investigated whether MPD precedes left ventricular systolic dysfunction and tested the hypothesis that prolonged use of dipyridamole (DIPY) could reduce MPD in an experimental model of CCC in hamsters.**

Methods and results. **We investigated female hamsters 6-months after *T. cruzi* infection (baseline condition) and control animals, divided into *T. cruzi*-infected animals treated with DIPY (CH + DIPY) or placebo (CH + PLB); and uninfected animals treated with DIPY (CO + DIPY) or placebo (CO + PLB). The animals were submitted to echocardiogram and rest SPECT-Sestamibi-Tc99m myocardial perfusion scintigraphy. Next, the animals were treated with DIPY (4 mg/kg bid, intraperitoneal) or saline for 30 days, and reevaluated with the same imaging methods. At baseline, the CH + PLB and CH + DIPY groups showed larger areas of perfusion defect (13.2 ± 13.2% and 17.3 ± 13.2%, respectively) compared with CO + PLB and CO + DIPY (3.8 ± 2.2% e 3.5 ± 2.7%, respectively), $P < .05$. After treatment, we observed: reduction of perfusion defects only in the CH + DIPY group (17.3 ± 13.2% to 6.8 ± 7.6%, $P = .001$) and reduction of LVEF in CH + DIPY and CH + PLB groups (from 65.3 ± 9.0% to 53.6 ± 6.9% and from 69.3 ± 5.0% to 54.4 ± 8.6%, respectively, $P < .001$). Quantitative histology revealed greater extents of inflammation and interstitial fibrosis in both**

All editorial decisions for this article, including selection of reviewers and the final decision, were made by guest editor Alberto Cuocolo, MD.

Reprint requests: Marcus Vinícius Simões, PhD, Medical School of Ribeirao Preto, University of São Paulo, Sao Paulo, Brazil; *msimoes@fmrp.usp.br*

1071-3581/$34.00

Chagas groups, compared with control group ($P < .001$), but no difference between Chagas groups ($P > .05$).

Conclusions. **The prolonged use of DIPY in this experimental model of CCC has reduced the rest myocardial perfusion defects, supporting the notion that those areas correspond to viable hypoperfused myocardium. (J Nucl Cardiol 2019;26:1569–79.)**

Key Words: Chagas cardiomyopathy • coronary microcirculation • dipyridamole • ventricular dysfunction • hamsters

Abbreviations	
CCC	Chronic Chagas cardiomyopathy
MPD	Myocardial perfusion defects
DIPY	Dipyridamole
PLB	Placebo
LV	Left ventricle
LVEDD	Left ventricle end diastolic dimension
LVESD	Left ventricle end systolic dimension
LVEF	Left ventricular ejection function
PD	Perfusion defects
SPECT	Single photon emission computerized tomography

See related editorial, pp. 1580–1583

INTRODUCTION

Chagas disease is still endemic in many regions of Latin America, where from 8 to 10 million people are estimated to be infected,[1] and represents an emerging public health issue in nonendemic countries such as the United States and the European and Asian countries.[2,3]

The most relevant clinical manifestation of the disease in its chronic phase is a dilated cardiomyopathy arising at about 2 to 3 decades after the initial infection. An intriguing aspect of the pathogenesis of chronic Chagas cardiomyopathy (CCC) involves which predominant injuring mechanisms lead to such a delayed development of myocardial damage.[4] The main pathogenic mechanisms considered to be central in this process are myocardial aggression depending on persistently low intensity but incessant parasitism[5] and myocardial injury mediated by the immune system.[6]

Besides the above, clinical studies have demonstrated a high rate of ischemic perfusion defects (30 to 50%) in chronic Chagas disease patients with normal sub-epicardial coronary arteries, suggesting that myocardial perfusion disturbances occurring due to microvascular dysfunction may also take part in the myocardial lesion process.[7–9] This hypothesis is further supported by necroscopic studies showing topographic correlation between coronary microvascular obstruction and ischemic myocardial lesions in CCC patients.[10,11]

Previous results of our research group showed rest myocardium perfusion defects are detected when using in vivo imaging in experimental model of CCC in hamsters. These rest myocardium perfusion defects (MPD) were topographically related to increased myocardial inflammation and regional systolic dysfunction but not with regional fibrosis, raising the possibility to represent areas of viable myocardium with resting hypoperfusion.[12]

Thus, to understand those findings in greater depth, the present study aimed at investigating whether the MPD precede the LV systolic dysfunction in the experimental model of CCC in hamsters. In addition, we also tested the hypothesis that the prolonged use of a coronary vasodilator agent, viz., dipyridamole, could ameliorate the rest MPD in this experimental model of CCC.

METHODS

Experimental Animals

Twelve-week-old female hamsters (*Mesocricetus auratus*) (Anilab—Animais de Laboratório Criação e Comércio Ltda, Paulínia/SP, Brasil) were used for the study. The animals were maintained in a climatically controlled environment on a 12-h light/dark cycle with free access to food and standard chow. All procedures and protocols were approved by the Animal Research Ethics Committee of the Institution (Protocol n° 028/2014).

Experimental Protocol

The animals of the Chagas group were infected intraperitoneally with 3.5×10^4 trypomastigote forms of *T. cruzi* Y-strain. Control animals were inoculated with the same volume of saline solution.

Six months after *T. cruzi* infection or saline injection for controls, all animals were submitted to baseline imaging studies, including high-resolution myocardial perfusion-SPECT and echocardiography. This time window was chosen based on previous works indicating that at 6 months after infection, the animals present no significant LV systolic dysfunction.[13]

The animals were then divided into four groups: (1) Chagas + dipyridamole (CH + DIPY, $n = 15$): chronically *T. cruzi*-infected animals treated with dipyridamole; (2) Chagas + placebo (CH + PLB, $n = 15$): chronically *T. cruzi*-infected animals treated with placebo; (3) Control + dipyridamole (CO + DIPY, $n = 10$): noninfected animals treated

with dipyridamole; and (4) Control + placebo (CO + PLB, $n = 10$): noninfected animals treated with placebo.

The animals treated with dipyridamole received an intraperitoneal injection of 4 mg/kg twice a day for 30 days. This dose was chosen based on previous studies investigating the effect of dipyridamole in rodent microcirculation.[14,15] Placebo-treated animals were injected intraperitoneally with the same volume of saline solution.

In the posttreatment evaluation, the animal underwent the same imaging methods used at the baseline, which was followed by euthanasia and collection of blood samples and heart tissue. The confirmation of chronic Chagas infection was performed by detection of anti-*T. cruzi* antibodies in the sera of the infected hamsters with a Western blot assay with the TESA fraction of secreted *T. cruzi* antigens employing anti-hamster IgG conjugated to horseradish peroxidase as the secondary antibody as previously described.[16]

Echocardiographic Assessment of Ventricular Remodeling and Function

After sedation with ketamine and xylazine (100 and 10 mg/kg), the echocardiogram was recorded using the high-resolution Philips HD11XE two-dimensional echocardiography system (Philips, Andover, MA) provided with a 15-MHz high-frequency linear transducer. Using the parasternal window to obtain long-axis and short-axis images of the LV at the papillary level, M-mode images were used for the measurement of interventricular septum and LV posterior wall thickness, as well as LV end diastolic (LVEDD) systolic (LVESD) dimensions. The diastolic diameter of the LV was measured in the maximum ventricular diastolic dimension, and the systolic LV dimension was obtained during maximum inward motion of the septum and posterior wall. LVEF was calculated applying the Teichholz formula.

The images were recorded by an echocardiographer experienced in lab work with small animals who was blind to the group to which the animals belonged, for the offline analysis at the end of the study.

All measures represented the means of at least five consecutive cardiac cycles using the same projection, transducer positions, and angulation and in the same frozen image frame.

High-Resolution Myocardial Perfusion SPECT

Images were acquired with a high-resolution imaging system based on pinhole collimators coupled to a gamma camera of clinical use (BrightView XCT; Philips Medical Systems Inc., Cleveland, OH) that has recently been validated.[17,18] For image acquisition, the animals were anesthetized with 3% isoflurane, and 555 MBq of Sestamibi-Tc99m was injected into the sublingual vein. One hour after injection of the radiopharmaceutical, the animals were anesthetized with ketamine (100 mg/Kg) and xylazine (10 mg/kg), intramuscular, and positioned in a cylindrical support that permitted to rotate the animals to sequential angular positions in the image acquisition system. Forty projections equally spaced over 360° were acquired, 30 s/projection, using a 128 × 128 acquisition matrix.

The dipyridamole or placebo administration was kept in all experimental groups until the radiotracer injection. The animals of DIPY groups received the last dose of dipyridamole around 8 hours before the radiotracer injection; thus, images were performed under the effect of dipyridamole.

The images were exported in DICOM format and were processed to obtain the three-dimensional model of radiopharmaceutical distribution in the target organ using a dedicated reconstruction software.[17]

Analysis of myocardial perfusion was based on the construction of a polar map generated with the previously validated software for the quantitative assessment of defect areas.[18] Perfusion defects (PD) were identified by pixels with uptake below 50% in relation to the pixels of maximum uptake value. The results of quantitation are reported as percent area of perfusion defect in relation to total LV surface. LV segmentation into a 13-segment model (6 basal, 6 mid-ventricular and 1 apical) was used for the topographic correlation of the perfusion defect areas with the results of histopathologic studies.

Histopathology

After deep anesthesia, the chest was opened, and the animals were sacrificed by exsanguination. The heart was excised and washed in PBS solution, and basal vessels and atria were discarded.

For histopathologic analysis, short-axis sections were obtained at three ventricular levels (basal, mid-ventricular, and apical). Slices were scanned and analyzed using a digital pathology system consisting of a digital scanner (Scanscope CS System; Aperio Technologies Inc., Vista, CA, USA).

Samples with areas ranging from 1.5 to 2 mm^2 were used for all analyses, maintaining a topographic correlation with the in vivo imaging exams. The samples were stained with hematoxylin–eosin for quantitative analysis of inflammatory intensity by automatic counting of the number of clusters of mononuclear cells per mm^2. The extent of fibrosis was quantitated using picrosirius staining, and measured as percent area of interstitial and perivascular fibrosis.

Statistical Analysis

Continuous variable data are reported as mean ± standard deviation, and nominal variables are reported as absolute (n) and relative (%) frequency.

The Shapiro–Wilk test was used to determine Gaussian distribution of variables. We used the One-way Analysis of Variance (ANOVA) for the simultaneous comparison among the four experimental groups of the baseline means of myocardial perfusion defect areas, echocardiography variables, and for the histopathological results of inflammation performed after treatment. Kruskal–Wallis was used for the simultaneous comparison of fibrosis extent, which presented non-Gaussian distribution, at the end of study.

A mixed ANOVA for repeated measures was used to assess interaction (main effect) between the experimental groups (between-subject effect) and time (within-subject effect) on LVEF, LVEDD, and myocardial perfusion defect areas. Greenhouse–Geisser conservative *F*-test was used to take into account lack of compound symmetry when appropriate. Where a statistically significant interaction was found, simple effect tests were performed to evaluate differences between pre- and posttreatment values into each experimental group.

The level of significance was set at $P < .05$, two-tailed in all analyses.

Statistical analysis was performed using Stata, version 14.2 (StataCorp, College Station, TX, USA).

RESULTS

General Aspects and Mortality

During treatment, five infected animals died, three from the placebo group and two from the dipyridamole group. In the control group, one animal receiving dipyridamole died. Only surviving animals were used for statistical analysis.

LV Function

The results of the echocardiogram and myocardial perfusion-SPECT at baseline and posttreatment evaluation are presented in Table 1.

The echocardiography parameters were similar for all groups at baseline evaluation, ANOVA—$P > .05$.

Repeated-measures ANOVA of LVEF showed a significant interaction between the experimental groups and time (pre- and posttreatment time interval), $P = .016$. In a post hoc test of simple effects, posttreatment LVEF was reduced in comparison with pretreatment LVEF in both Chagas group (CH + PLB and CH + DIPY), $P < .001$ for both comparisons. No difference was detected in the control groups, $P > .05$. No significant interaction between the groups and time on LVEDD was found, $P = .133$.

Myocardium Perfusion

Thirteen of the 25 infected animals (52%) showed significant areas of perfusion defects compared with control, ANOVA—$P < .05$. Of the 325 segments analyzed in both *T. cruzi* infected groups, 64 (20%) showed perfusion defects. Among the 13 animals with perfusion defects, the segments most frequently involved were apical (100%), anterior-basal (69%), anterior-basal septum (69%), inferior-basal septum (62%), and mid-inferior septum (54%).

Repeated-measures ANOVA of area of perfusion defects showed a significant interaction between the experimental groups and time (pre- and posttreatment time interval), $P = .036$. A significant reduction of the area of perfusion defects was observed only in the infected group treated with dipyridamole (Table 1, Figures 1, 2B, $P < .001$). In the CH + PLB group and in the control noninfected groups, the areas of perfusion defects were similar at baseline and in the posttreatment period (Table 1, Figures 1, 2A).

Table 1. Baseline and posttreatment results of echocardiographic and myocardial perfusion studies for each experimental group

Variables	Control + PLB ($n = 10$)	Control + DIPY ($n = 9$)	Chagas + PLB ($n = 12$)	Chagas + DIPY ($n = 13$)	*P* (ANOVA)
LVEF (%)					
Baseline	65.1 ± 9.8	63.0 ± 5.3	69.3 ± 5.0	65.3 ± 9.0	$P = .016$
Post treatment	60.0 ± 8.8	59.3 ± 8.9	54.4 ± 8.6*	53.6 ± 6.9*	
LVEDD (cm)					
Baseline	0.7 ± 0.06	0.6 ± 0.06	0.6 ± 0.03	0.7 ± 0.05	$P = .133$
Post treatment	0.7 ± 0.12	0.6 ± 0.10	0.7 ± 0.08	0.8 ± 0.06	
PD (%)					
Baseline	3.8 ± 2.2	3.5 ± 2.7	13.2 ± 13.2	17.3 ± 13.2	$P = .036$
Post treatment	5.5 ± 3.2	2.9 ± 3.3	10.5 ± 10.0	6.8 ± 7.6*	

Data are reported as mean ± standard deviation. The *P* values refer to the results for the main effect of the mixed ANOVA for repeated measures test

LVEF left ventricular ejection fraction; *LVEDD* left ventricular end diastolic dimensions; *PD* Perfusion defects; *DIPY* dipyridamole; *PLB* placebo

*$P < 0.001$ vs baseline, simple effect posttest

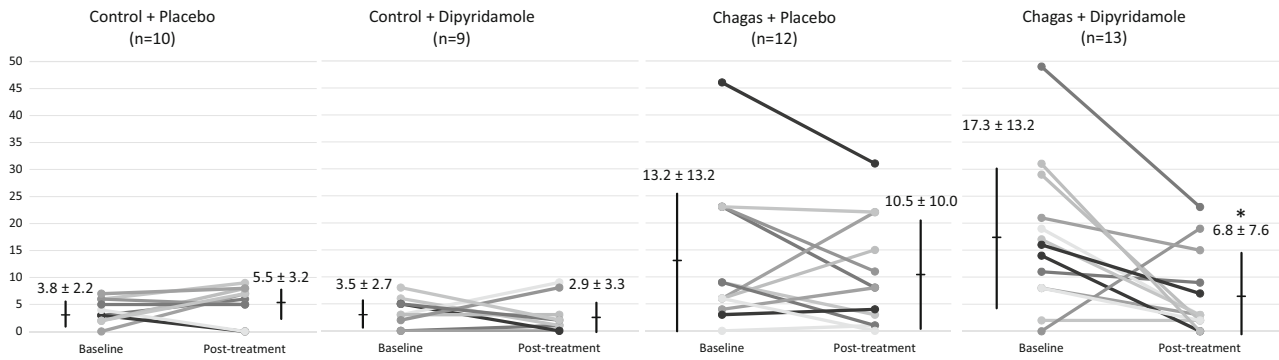

Figure 1. Line graphs representing the values of myocardium perfusion defects areas obtained for each experimental group at baseline and posttreatment with dipyridamole or placebo. $*P < 0.001$ vs baseline, simple effect posttest.

Histopathological Analysis

A significant number of the Chagas animals exhibited important chamber dilation with reduced LV wall thickness. However, no significant areas of transmural fibrosis were detected. An intense focal inflammatory infiltrate with mononuclear cells was usually detected in sub-epicardial or perivascular regions. Most animals exhibited mild multifocal myocarditis. Preserved fibers were detected in the control animals (Figure 3A).

The intensity of the inflammatory infiltrate estimated by the number of mononuclear cells and the extent of fibrosis in each experimental group are reported in Figure 3B. A larger number of clusters of mononuclear inflammatory cells were detected in both Chagas groups compared with controls, ANOVA—$P < .0001$. There was no significant difference between the CH + DIPY and CH + PLB groups.

The extent of fibrosis was greater in the CH + DIPY and CH + PLB groups compared with the CO + PLB group, Kruskal–Wallis test—$P < .001$. We found no difference of fibrosis extent between the groups of infected animals treated with placebo or dipyridamole ($P > .05$, Dunn's posttest).

DISCUSSION

The main results of the present study show that rest myocardium perfusion defects are frequent and precede the development of LV systolic dysfunction in this experimental model of CCC in hamsters. Notably, the areas with PD were not topographically related to regional myocardial fibrosis at the histopathology. The prolonged administration of dipyridamole, an antiplatelet and vasodilator agent of the coronary microcirculation, was associated with a significant reduction of the resting myocardial perfusion defects.

The Experimental Model of CCC

In the baseline condition (6-months after *T. cruzi* infection), both groups of *T. cruzi* infected animals showed LVEF and LVEDD values similar to those observed in the control groups. These results indicated that infected animals at this time window of 6-months after infection had not yet developed significant LV systolic dysfunction in this intermediate stage of experimental CCC development, despite the detection of low-grade chronic myocarditis. This finding agrees with previous reports by Bilatte et al., in which significant LV dysfunction was first detected in the time window of 8-months after infection.[13,19] Thus, it is plausible to consider that, at baseline evaluation, with regard to LV systolic function, the infected hamsters were in an evolutive phase corresponding to the indeterminate form seen in humans with CCC.[20]

It is relevant to mention that only female animals were used in this study as previous reports indicated that the parasitism and disease progression were more homogenous and predictable in females.[21] However, it is also noteworthy to mention that CCC in humans presents a more aggressive course in males.[22]

Again, in agreement with previous reports, we observed in both infected groups receiving placebo or DIPY a substantial progression of myocardial dysfunction between the baseline and posttreatment evaluations, characterized by a significant reduction of LVEF, resembling the natural evolution of CCC.[13]

In the histopathological analysis, both groups of Chagas animals presented a larger extent of inflammatory infiltrates, compared with the control groups. Moreover, both infected groups presented similar extent of fibrosis that was larger than the amount observed in the CO + PLB group. These results agree with previous studies in this same phase of CCC evolution in hamsters.[12,19]

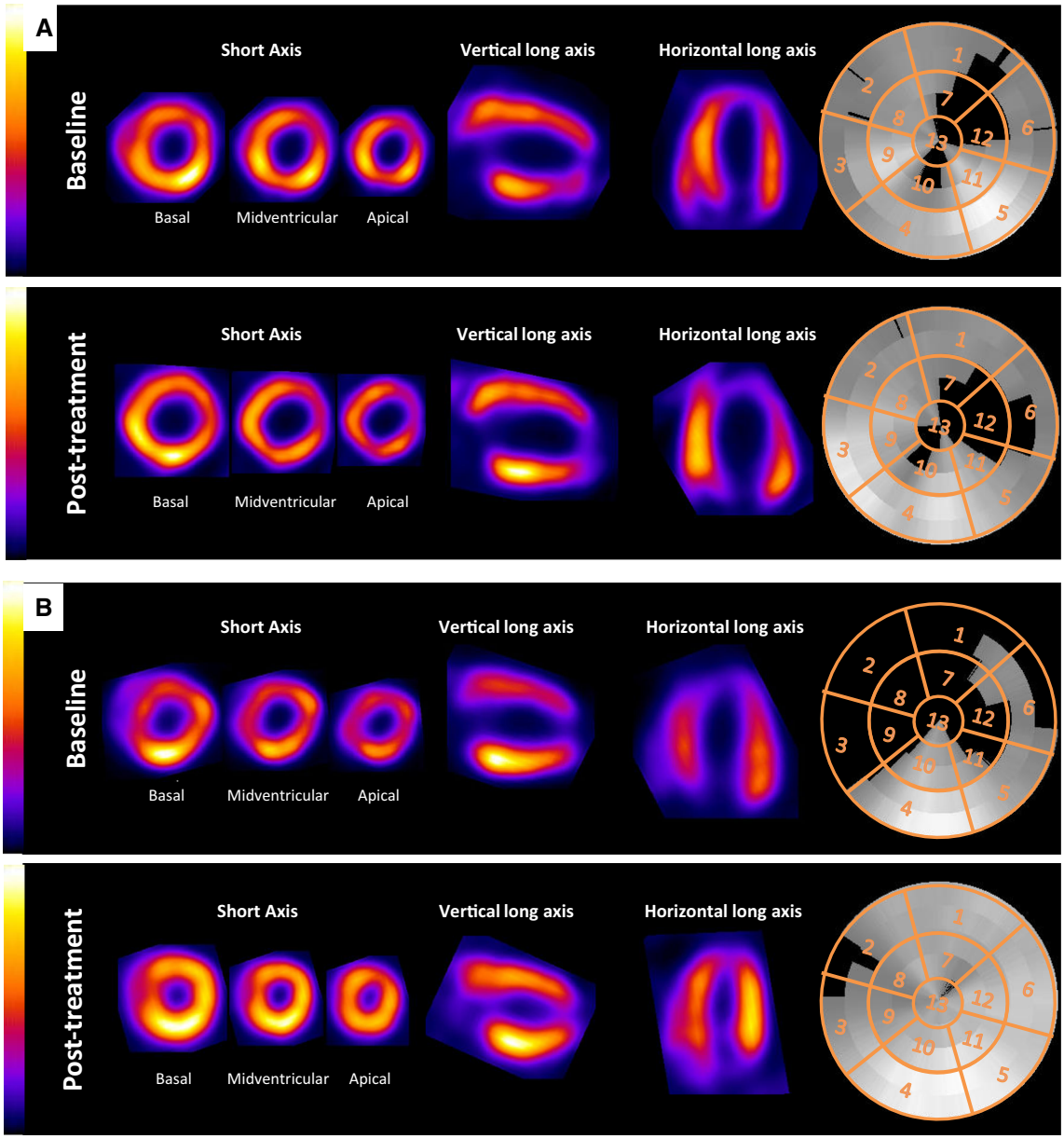

Figure 2. Illustrative images of the study of myocardial perfusion at baseline and posttreatment in an infected animal treated with placebo (**A**) or DIPY (**B**). Representative sections of tomographic images (SPECT) are shown. The images were obtained at three levels of the left ventricular cavity (basal, mid-cavity, and apical) and on vertical and horizontal long axes, with the resulting polar map shown in the right side of the figure. The placebo-treated animal presented at baseline severe perfusion defects in the anterior-lateral and apical walls that persisted during the posttreatment evaluation. The dipyridamole-treated animal presented a large severe perfusion defect involving the septal, anterior, lateral, and apical wall at the baseline evaluation, with a striking reduction of perfusion impairment in the images acquired in the posttreatment evaluation.

However, we found no difference in the comparison among the infected groups and the CO + DIPY. This result probably reflects the only slightly increased amount of fibrosis in the infected animals in this intermediate phase of CCC evolution, in which the inflammation predominates over the interstitial fibrosis.[19]

Myocardial Perfusion Disturbances

At the baseline evaluation, 6-months after experimental *T. cruzi* infection, we observed that 52% of the animals had resting myocardial perfusion defects. Notably, the histological analysis in the same

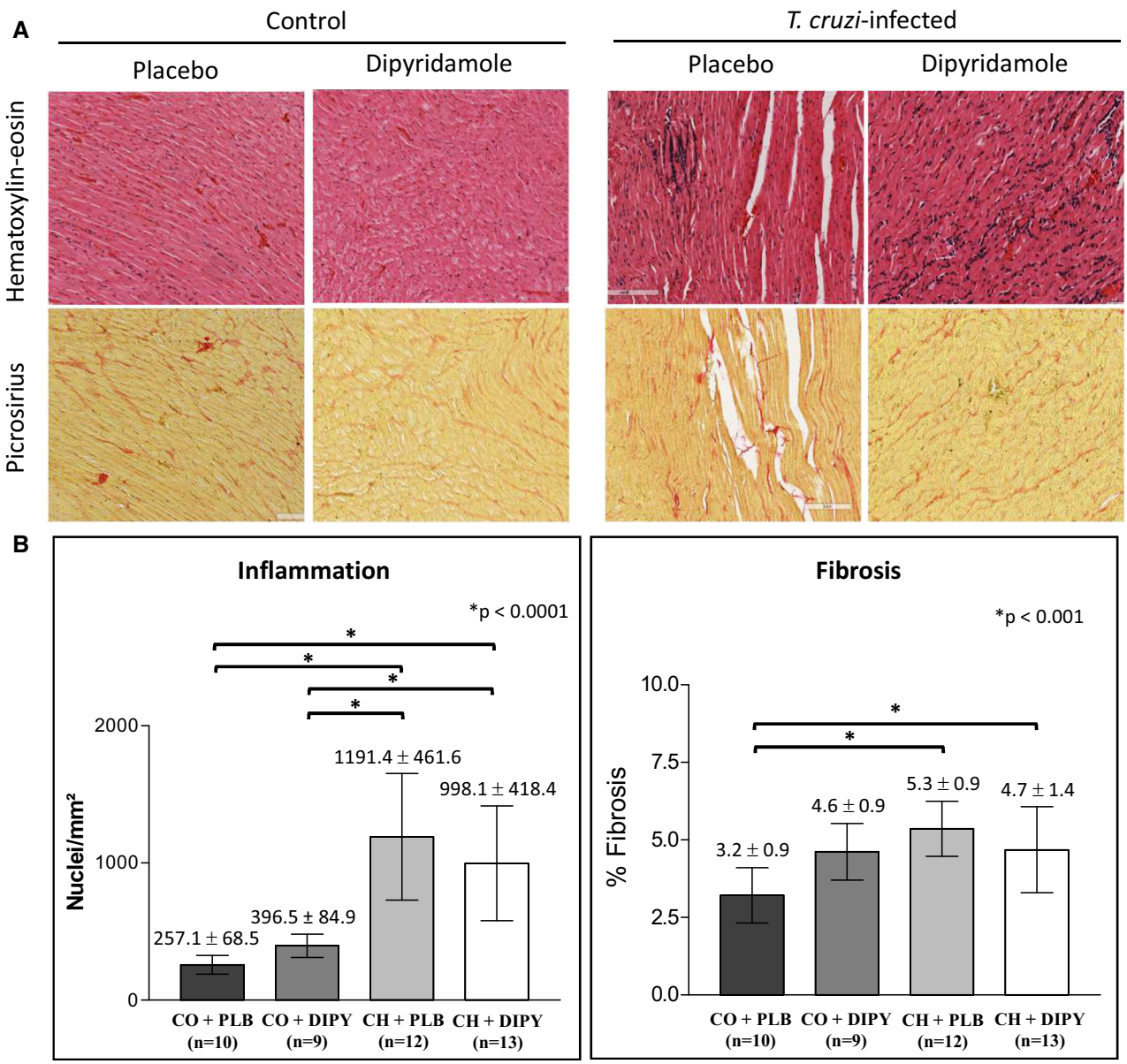

Figure 3. A Representative histological sections stained with HE (upper panels) and with picrosirius (lower panels) from each experimental group. The histological samples of infected animals show focal points of a diffuse mononuclear inflammatory infiltrate and fibrosis, with similar intensity in both placebo and dipyridamole groups. **B** Bar graphs representing the results of quantitative analysis of inflammation and fibrosis for each experimental group. Data are reported as mean ± standard deviation. *DIPY*, dipyridamole, *PLB*, placebo. The p value of inflammation refers to the One-way Analysis of Variance (ANOVA) test with Tukey posttest, and the *P* value of fibrosis refers to Kruskal–Wallis test with Dunn's posttest.

topography of the LV wall showed no transmural or coalescent areas of fibrosis. Thus, it is plausible to interpret these perfusion defects as being secondary to intense resting myocardial hypoperfusion, possibly indicating the presence of microvascular dysfunction in this CCC model.

The most frequently affected myocardial region was the apical segment. It is relevant to consider that some extent of these apical perfusion defects can be related to artifacts caused by partial volume effect due to apical thinning and also to the high mobility of the apex in small rodents' hearts. However, all the apical perfusion

defects in infected animals were larger than those mild ones observed in controls. Moreover, other myocardial regions were also frequently affected by perfusion defects, indicating the presence of nonartifactual perfusion derangements in infected animals.

In the present study, we obtained high-resolution myocardial perfusion images in hamsters by means of an imaging system based on the adaptation of a pinhole collimator to a gamma camera designed for clinical use. This was needed because the spatial resolution of conventional gamma cameras is not enough for imaging small animals, which present the size of about one-tenth of human-being size. The use of such a pinhole collimation system is a validated alternative to achieve high-resolution SPECT images in small animals.[17]

Our results agree with previous data obtained by our group using the same experimental model of CCC. In that previous study, 50% of the animals investigated in a later time window of cardiomyopathy progression (8 and 10 months after experimental *T. cruzi* infection) exhibited myocardial perfusion defects topographically correlated with changes in segmental LV wall motion and greater severity of global LV systolic dysfunction. In addition, in that study, the myocardial segments with perfusion defects were not topographically correlated with areas of increased regional fibrosis, but were associated with greater severity of myocardial inflammation.[12]

It is important to mention that alternative mechanisms to explain the reduction in the rest myocardial uptake of Sestamibi-Tc99 m might include an impairment of the radiotracer accumulation and/or an increased washout associated to mitochondrial dysfunction. In fact, previous studies have demonstrated that the myocardial accumulation and retention of Sestamibi is strongly dependent on the functional and structural mitochondrial integrity.[23] It is known that local myocardial production of inflammatory cytokines including IFN- γ and TNF- α is associated with iNOS production leading to morphological and functional changes in mitochondria, which could modify the uptake of the radiopharmaceutical.[24,25] Following this hypothesis, the Sestamibi-Tc99m uptake defects would indicate the presence of myocardial inflammation but not the occurrence of true myocardial perfusion defects. However, in our study, the prolonged administration of dipyridamole was associated with improvement of the Sestamibi-Tc99m uptake, despite no significant change in the inflammation extent assessed by the histopathological findings. Therefore, our results indicate that the observed Sestamibi-Tc99m uptake defects most probably correspond to reduction of myocardial perfusion at rest.

The interpretation of our present findings indicating that myocardial perfusion changes were caused by microvascular derangements is further supported by the results of clinical studies showing reversible and fixed defects in the myocardial perfusion scintigraphy in humans with CCC and angiographically normal coronary arteries, described by our and other groups of investigators.[7,9,20]

In contrast to our findings, one previous study using contrast echocardiography in naturally infected Chagas baboons did not find changes in the coronary microcirculation.[26] However, it is important to consider that in previous studies in CCC, both in humans and in our experimental model, only about 50% of the subjects present myocardial perfusion disturbance. In that study in Baboons, only four animals had developed CCC as documented by segmental wall motion impairment, resulting in a very small sample to conclude the absence of myocardial perfusion derangements. In addition, we must also consider that the evaluation method used, contrast Echocardiography, may present lower sensitivity compared with the myocardial perfusion scintigraphy for detecting microvascular disease.[27]

In addition, our results indicate that severe myocardium perfusion disturbances at rest precede the development of LV systolic dysfunction in this experimental model of CCC. These findings are in accordance with previous observations showing disarrangements of myocardium perfusion in humans with CCC but no apparent myocardial dysfunction [20] Furthermore, clinical studies also showed that areas with reversible myocardial perfusion defects are topographically related to late development of regional fibrosis and segmental wall motion impairment in CCC patients.[9]

The Effects of Dipyridamole

Our results showed a significant effect of prolonged dipyridamole administration leading to a marked reduction of resting MPD in this experimental model of CCC. To the best of our knowledge, this is the first study to demonstrate the beneficial effect of dipyridamole in improving myocardial perfusion in an experimental model of dilated cardiomyopathy.

These results agree with the effects expected from the pharmacological action of dipyridamole. This drug is a vasodilator of the microcirculation, acting by inhibiting the adenosine transporter and the consequent elevation of its plasma levels.[28,29] Adenosine binds to endothelial and muscle cell receptors of the arteriolar wall, causing relaxation and consequent vasodilation. The combined effects of vasodilation and platelet antiaggregation are considered to be the main factors

responsible for the improved tissue perfusion observed with the use of dipyridamole.[29]

The pharmacologic action of dipyridamole also includes the inhibition of phosphodiesterases-5 and 6,[30,31] causing an increase of both cAMP and cGMP levels, with a consequent increase of nitric oxide release, contributing to arteriolar vasodilation and inhibition of platelet aggregation.[29,32,33] In addition, dipyridamole has been reported to be related to the induction of capillary endothelial cell proliferation and to capillary neoformation in the rat heart.[14,15] Studies using a model of hind limb ischemia in mice demonstrated improved collateral arterial perfusion and restoration of blood flow in animals treated with dipyridamole, effects associated with increased perfusion through the microcirculation secondary to the increase in vascular density and cell proliferation.[34]

The mechanism leading to the myocardial perfusion disturbance at the microvascular level in CCC is postulated to include inflammatory injuries and thickening of the vascular walls that would lead to the obstruction of the small coronary arteriolar branches, to the formation of platelet plugs and to endothelial injury, associated with an increased production of endothelin and of inflammatory cytokines,[10,35,36] in addition to a possible occurrence of abnormal vasoreactivity and coronary arteriolar spasms.[37]

It is plausible to assume that the effect of dipyridamole in reducing the perfusion disturbances in this experimental model may have been mediated by the action of the drug on several of the mechanisms mentioned above, mainly by inhibition of the formation of platelet plugs, and reversal of endothelial dysfunction and of arteriolar spasms. In addition, the improved myocardial perfusion may also have been due to the neoangiogenic effect of adenosine.[34]

Our quantitative histopathology findings showed comparable degrees of myocardial inflammation and fibrosis in both infected groups treated with placebo or dipyridamole, indicating that the effect of prolonged dipyridamole in reducing MPD was not due to a reduction of myocardial inflammation, eventually associated to the drug effect.

In the control groups the extent of inflammation was also comparable, but in a lower grade, than that observed in the infected animals. These findings were consistent with a neutral effect of dipyridamole over inflammation.

One could argue that the apparent reduction of the perfusion defects could happen in consequence of a hemodynamic effect of dipyridamole, causing arterial vasodilation and facilitating the LV systolic function and hence producing an increased regional LV wall thickening that could contribute for the apparent reduction of the MPD. However, this explanation does not seem plausible, as there was no significant difference in the LVEF or LV diameters in both groups, control or infected, after treatment with DIPY compared with the respective placebo groups. These results indicate that prolonged dipyridamole administration cause no significant hemodynamic effect capable of inducing changes in LV volume, wall thickness or systolic function.

Thus, in summary, our results indicate that prolonged use of dipyridamole improves the myocardial perfusion in this model of CCC.

In essence, the fact that dipyridamole led to amelioration of the perfusion defects in *T. cruzi* infected animals further supports the notion that the observed rest myocardium perfusion defects at baseline correspond to viable myocardium. In addition, these findings corroborate the presence of coronary microvascular derangements in this model of CCC.

The current results can lend support for the future development of prospective investigations using coronary vasodilator drugs, such as dipyridamole, for the treatment of microvascular myocardial perfusion disturbance in CCC patients, evaluating its potential impact on the course of myocardial systolic dysfunction.

NEW KNOWLEDGE GAINED

Our results show that coronary microvascular perfusion disturbance is an important feature in experimental CCC preceding the development of LV systolic dysfunction. This aspect may have important implications for the clinical scenario, where myocardial perfusion scintigraphy may play a relevant role in the early detection of CCC and in the monitoring of its evolution.[38] It also lends support to the notion that myocardium perfusion disturbance may be a target for therapeutic interventions in human Chagas disease.

LIMITATIONS

In the present study, we performed no arterial blood pressure assessment that could be useful to verify the hemodynamic effects of prolonged dipyridamole. It is also important to acknowledge that the assessment of myocardial perfusion using SPECT technique provides a qualitative and comparative evaluation of myocardial perfusion, but not a quantitative estimate of the myocardial perfusion. This may have caused an underestimation of the myocardial perfusion disturbance that could be more accurately evaluated by other quantitative imaging techniques such as PET.

In addition, it is noteworthy that a proportion of the infected animals treated with placebo also presented reduction of the perfusion defects between the baseline

and posttreatment (Figure 1). This finding suggests the occurrence of spontaneous changes in the magnitude of the microvascular abnormalities over time, or a low reproducibility of the myocardial perfusion assessment in this model of CCC.

We did not perform evaluation of the diastolic function, as we used Echocardiography equipment that could not provide adequate Doppler images. It is relevant to recognize that diastolic dysfunction would be an important parameter to monitor the course of myocardial dysfunction in CCC.

CONCLUSIONS

The present results show that myocardium perfusion disturbance is frequent in experimental CCC and precedes the development of myocardium systolic dysfunction. The prolonged administration of dipyridamole in chronically *T. cruzi*-infected hamsters is associated with a significant reversion of resting myocardial perfusion defects, thus indirectly indicating the presence of viable myocardium in those hypoperfused myocardial segments, and confirming the occurrence of microvascular dysfunction in CCC.

These findings lend support for future prospective studies testing the impact of drugs targeting the myocardial perfusion derangement over the myocardial systolic dysfunction progression in CCC.

Disclosures

Denise Mayumi Tanaka, Luciano Fonseca Lemos de Oliveira, José Antônio Marin-Neto, Minna Moreira Dias Romano, Eduardo Elias Vieira de Carvalho, Antonio Carlos Leite de Barros Filho, Fernando Fonseca França Ribeiro, Jorge Mejia Cabeza, Carla Duque Lopes, Camila Godoy Fabricio, Norival Kesper, Henrique Turin Moreira, Lauro Wichert-Ana, André Schmidt, Maria de Lourdes Higuchi, Edécio Cunha-Neto, and Marcus Vinícius Simões declare that they have no conflict of interest.

Funding

This study was supported by a research grant from Fundação de Apoio à Pesquisa do Estado de São Paulo (FAPESP—Process: 2014/07722-4) and Fundação de Apoio ao Ensino Pesquisa e Assistência do Hospital das Clínicas (FAEPA).

References

1. Organización Panamericana de la Salud. Organización Panamericana de la Salud. Estimación cuantitativa de la enfermedad de Chagas en las Américas. Washington, DC; 2006.
2. Nunes MC, Dones W, Morillo CA, Encina JJ, Ribeiro AL. Council on Chagas Disease of the Interamerican Society of C. Chagas disease: An overview of clinical and epidemiological aspects. J Am Coll Cardiol 2013;62:767-76.
3. Gascon J, Bern C, Pinazo MJ. Chagas disease in Spain, the United States and other non-endemic countries. Acta Trop 2010;115:22-7.
4. Marin-Neto JA, Cunha-Neto E, Maciel BC, Simoes MV. Pathogenesis of chronic Chagas heart disease. Circulation 2007;115:1109-23.
5. Benvenuti LA, Roggerio A, Freitas HF, Mansur AJ, Fiorelli A, Higuchi ML. Chronic American trypanosomiasis: Parasite persistence in endomyocardial biopsies is associated with high-grade myocarditis. Ann Trop Med Parasitol 2008;102:481-7.
6. Borges DC, Araujo NM, Cardoso CR, Lazo Chica JE. Different parasite inocula determine the modulation of the immune response and outcome of experimental Trypanosoma cruzi infection. Immunology 2013;138:145-56.
7. Hagar JM, Rahimtoola SH. Chagas' heart disease in the United States. N Engl J Med 1991;325:763-8.
8. Marin-Neto JA, Marzullo P, Marcassa C, Gallo Junior L, Maciel BC, Bellina CR, et al. Myocardial perfusion abnormalities in chronic Chagas' disease as detected by thallium-201 scintigraphy. Am J Cardiol 1992;69:780-4.
9. Hiss FC, Lascala TF, Maciel BC, Marin-Neto JA, Simoes MV. Changes in myocardial perfusion correlate with deterioration of left ventricular systolic function in chronic Chagas' cardiomyopathy. JACC Cardiovasc Imaging 2009;2:164-72.
10. Torres CM. Arteriosclerosis of the fine arterial branches of the myocardium (Chagas' coronaritis) & focal myocytolysis in chronic Chagas' heart disease. Hospital (Rio J) 1958;54:597-610.
11. Higuchi ML. Endomyocardial biopsy in Chagas' heart disease: pathogenetic contributions. Sao Paulo Med J 1995;113:821-5.
12. Oliveira LFL, Carvalho EEV, Romano MMD, Mejia J, Tanaka DM, Abdalla DR et al. Regional myocardial perfusion disturbance in experimental model of chronic Chagas cardiomyopathy. In: European Heart Journal European Society of Cardiology Congress. Barcelona, Spain; 2017. p. 5413.
13. Bilate AM, Salemi VM, Ramires FJ, de Brito T, Silva AM, Umezawa ES, et al. The Syrian hamster as a model for the dilated cardiomyopathy of Chagas' disease: a quantitative echocardiographical and histopathological analysis. Microbes Infect 2003;5:1116-24.
14. Mall G, Schikora I, Mattfeldt T, Bodle R. Dipyridamole-induced neoformation of capillaries in the rat heart. Quantitative stereological study on papillary muscles. Lab Investig 1987;57:86-93.
15. Mattfeldt T, Mall G. Dipyridamole-induced capillary endothelial cell proliferation in the rat heart–a morphometric investigation. Cardiovasc Res 1983;17:229-37.
16. Umezawa ES, Nascimento MS, Kesper N Jr, Coura JR, Borges-Pereira J, Junqueira AC, et al. Immunoblot assay using excreted-secreted antigens of Trypanosoma cruzi in serodiagnosis of congenital, acute, and chronic Chagas' disease. J Clin Microbiol 1996;34:2143-7.
17. Mejia J, Galvis-Alonso OY, Castro AA, Braga J, Leite JP, Simoes MV. A clinical gamma camera-based pinhole collimated system for high resolution small animal SPECT imaging. Braz J Med Biol Res 2010;43:1160-6.
18. Oliveira LF, Mejia J, Carvalho EE, Lataro RM, Frassetto SN, Fazan R Jr, et al. Myocardial infarction area quantification using high-resolution SPECT images in rats. Arq Bras Cardiol 2013;101:59-67.
19. Oliveira LFL, Romano MMD, Carvalho EEV, Mejia J, Salgado HC, Fazan R Jr, et al. Histopathological correlates of global and segmental left ventricular systolic dysfunction in experimental chronic chagas cardiomyopathy. J Am Heart Assoc 2016;5:e002786.

20. Simoes MV, Pintya AO, Bromberg-Marin G, Sarabanda AV, Antloga CM, Pazin-Filho A, et al. Relation of regional sympathetic denervation and myocardial perfusion disturbance to wall motion impairment in Chagas' cardiomyopathy. Am J Cardiol 2000;86:975-81.
21. Schuster JP, Schaub GA. Experimental Chagas disease: the influence of sex and psychoneuroimmunological factors. Parasitol Res 2001;87:994-1000.
22. Assuncao AN Jr, Jerosch-Herold M, Melo RL, Mauricio AV, Rocha L, Torreao JA, et al. Chagas' heart disease: gender differences in myocardial damage assessed by cardiovascular magnetic resonance. J Cardiovasc Magn Reson 2016;18:88.
23. Hayashi D, Ohshima S, Isobe S, Cheng XW, Unno K, Funahashi H, et al. Increased (99 m)Tc-Sestamibi washout reflects impaired myocardial contractile and relaxation reserve during dobutamine stress due to mitochondrial dysfunction in dilated cardiomyopathy patients. J Am Coll Cardiol 2013;61:2007-17.
24. Tatsumi T, Matoba S, Kawahara A, Keira N, Shiraishi J, Akashi K, et al. Cytokine-induced nitric oxide production inhibits mitochondrial energy production and impairs contractile function in rat cardiac myocytes. J Am Coll Cardiol 2000;35:1338-46.
25. Ferreira LR, Frade AF, Baron MA, Navarro IC, Kalil J, Chevillard C, et al. Interferon-gamma and other inflammatory mediators in cardiomyocyte signaling during Chagas disease cardiomyopathy. World J Cardiol 2014;6:782-90.
26. Zabalgoitia M, Ventura J, Lozano JL, Anderson L, Carey KD, Hubbard GB, et al. Myocardial contrast echocardiography in assessing microcirculation in baboons with chagas disease. Microcirculation 2004;11:271-8.
27. Abdelmoneim SS, Basu A, Bernier M, Dhoble A, Abdel-Kader SS, Pellikka PA, et al. Detection of myocardial microvascular disease using contrast echocardiography during adenosine stress in type 2 diabetes mellitus: prospective comparison with single-photon emission computed tomography. Diab Vasc Dis Res 2011;8:254-61.
28. Bult H, Fret HR, Jordaens FH, Herman AG. Dipyridamole potentiates the anti-aggregating and vasodilator activity of nitric oxide. Eur J Pharmacol 1991;199:1-8.
29. Chakrabarti S, Freedman JE. Dipyridamole, cerebrovascular disease, and the vasculature. Vascul Pharmacol 2008;48:143-9.
30. Houslay MD, Sullivan M, Bolger GB. The multienzyme PDE4 cyclic adenosine monophosphate-specific phosphodiesterase family: intracellular targeting, regulation, and selective inhibition by compounds exerting anti-inflammatory and antidepressant actions. Adv Pharmacol 1998;44:225-342.
31. Nyby MD, Hori MT, Ormsby B, Gabrielian A, Tuck ML. Eicosapentaenoic acid inhibits Ca^{2+} mobilization and PKC activity in vascular smooth muscle cells. Am J Hypertens 2003;16:708-14.
32. Sakuma I, Akaishi Y, Fukao M, Makita Y, Makita MA, Kobayashi T, et al. Dipyridamole potentiates the anti-aggregating effect of endothelium-derived relaxing factor. Thromb Res Suppl 1990; 12:87-90.
33. Kukreja RC, Salloum FN, Das A, Koka S, Ockaili RA, Xi L. Emerging new uses of phosphodiesterase-5 inhibitors in cardiovascular diseases. Exp Clin Cardiol 2011;16:e30-5.
34. Venkatesh PK, Pattillo CB, Branch B, Hood J, Thoma S, Illum S, et al. Dipyridamole enhances ischaemia-induced arteriogenesis through an endocrine nitrite/nitric oxide-dependent pathway. Cardiovasc Res 2010;85:661-70.
35. Petkova SB, Huang H, Factor SM, Pestell RG, Bouzahzah B, Jelicks LA, et al. The role of endothelin in the pathogenesis of Chagas' disease. Int J Parasitol 2001;31:499-511.
36. Rossi MA, Goncalves S, Ribeiro-dos-Santos R. Experimental Trypanosoma cruzi cardiomyopathy in BALB/c mice. The potential role of intravascular platelet aggregation in its genesis. Am J Pathol 1984;114:209-16.
37. Factor SM, Cho S, Wittner M, Tanowitz H. Abnormalities of the coronary microcirculation in acute murine Chagas' disease. Am J Trop Med Hyg 1985;34:246-53.
38. Schwartz RG, Wexler O. Early identification and monitoring progression of Chagas' cardiomyopathy with SPECT myocardial perfusion imaging. JACC Cardiovasc Imaging 2009;2:173-5.